



Inorg. Chem. Res., Vol. 2, No. 2, 145-157, December 2019

DOI: 10.22036/icr.2020.219286.1058

Dye and Cobalt Electrolyte Interaction Effect on the Performance of Dye-Sensitized Solar Cell

Z. Parsa, P. Tahay, N. Rabiee and N. Safari*

Department of Chemistry, Shahid Beheshti University, Evin, 1983963113 Tehran, Iran

(Received 9 February 2020, Accepted 21 April 2020)

The effects of changing ligand structures of cobalt complexes as electrolytes on the performance of the dye-sensitized solar cell were investigated. In this paper, cobalt(II/III) tris(2,2'-bipyridine), cobalt(II/III) tris(4,4'-dimethyl-2,2'-bipyridine) and cobalt(II/III) tris(4,4'-dimethoxy-2,2'-bipyridine) complexes as electrolytes in conjugate with organic dye D149 were investigated to consider the correlation of the cobalt complexes structural on the efficiency of the dye-sensitized solar cell. The V_{oc} values of the prepared cells are related to the redox potential of their complexes and the maximum V_{oc} was observed with cobalt(II/III) tris(2,2'-bipyridine) electrolyte. The obtained results represented that the cobalt(II/III) tris(4,4'-dimethyl-2,2'-bipyridine) electrolyte has the highest efficiency in the solar cell compared with other cobalt complexes. These observed results have been interpreted by a possible interaction between the dye and cobalt complexes, which is more pronounced in the cobalt(II/III) tris(4,4'-dimethoxy-2,2'-bipyridine) cell. This interaction should be fine-tuning with the structure of dye and complex to increase the efficiency of the dye-sensitized solar cell. In addition, the results demonstrated that a thinner layer of the TiO_2 film decrease both the effects of mass transport issues and the charge recombination, therefore, it has significant advantages for cobalt electrolyte.

Keywords: Dye-sensitized solar cells, Redox mediator, Cobalt complexes, Interaction, Photovoltaic

INTRODUCTION

Dye-sensitized solar cell (DSSC) includes nanocrystalline metal oxides, photosensitizers, a counter electrode and an electrolyte with a redox couple [1-14]. The electrolyte, as a substantial part in DSSC, is responsible for the electron transport amongst oxidized dye and counter electrode [15,16]. The DSSC electrolyte should have proprieties such as long-term stability, high conductivity, positive potential compared to HOMO of the dye, ability to regenerate dye and no mass transport limitation [17]. An extensive range of molecular species and transition metal complexes have been investigated as redox couple in the electrolyte including I^-/I_3^- , Br^-/Br_3^- [18], $SCN^-/(SCN)_3^-$ [19], ferrocene/ferrocenium [20], copper (I/II) [21-24] and cobalt (II/III) [25,26]. I^-/I_3^- is used mostly as a redox couple in the

DSSC because of appropriate short circuit current and high stability [27,28]. Despite the excellent performances, it has some disadvantages, for instance, low redox potential, visible light absorption and its corrosive nature towards most metals [29-33]. With regards to these, cobalt polypyridine complexes can be replaced by Tri-iodide/iodide redox potential [34,35], which have tunable redox properties and noncorrosive nature towards the cathode [36-38].

The first report of cobalt electrolyte in DSSC was published with ruthenium (Ru) dyes and a maximum power conversion efficiency (PCE) about 2.2% was reached in 2001 [39]. Since then, many aspects of the cobalt complexes in DSSCs with Ru dyes, organic dyes and porphyrin dyes have been studied [30,37,40,41].

Hagfeldt *et al.* in 2010 recorded an efficient cell with cobalt bipyridyl as an electrolyte in combination with a bulky organic dye [42]. This promoted attentions in dye-

*Corresponding author. E-mail: n-safari@sbu.ac.ir

sensitized solar cell based on cobalt electrolytes in combination with organic and porphyrin dyes. Gratzel *et al.* have reported 13.0% efficiency by utilizing SM315 dye (a zinc-porphyrin dye) and Co(II/III) electrolyte [43].

It has found that one of the limitations of cobalt complexes is fast recombination amongst the injected electrons in the semiconductor and cobalt electrolyte. Another limitation for these complexes is diffusion impediment, which led to decrease in the fill factor of the DSSC. Therefore, an optimized condition for cobalt cells was supposed by using blocking groups on cobalt complexes and increasing TiO₂ pore size [44-46]. As a consequence, the structure of the cobalt complex and dye are very crucial for DSSCs performance. The recent progress is considered bulky substituents for suppressing recombination properties [47-49]. Also, to achieve an efficient cell, it is necessary to consider the proper dye with specific electrolyte, semiconductor and light intensity [50-56]. In fact, a small change in any component of DSSC can have a direct or indirect effect on other component and improve or reduce the efficiency [57-66].

In this study, we perused three complexes of cobalt(II/III) tris(2,2'-bipyridine), [Co(bpy)₃][PF₆]_{2/3}, cobalt(II/III) tris(4,4'-dimethoxy-2,2'-bipyridine), [Co(dMO-bpy)₃][PF₆]_{2/3} and cobalt(II/III) tris(4,4'-dimethyl-2,2'-bipyridine), [Co(dm-bpy)₃][PF₆]_{2/3} as electrolytes in DSSC devices. Both of the methyl- and methoxy-substituents are considered as donor group but methoxy is stronger electron donor compared with methyl. This work provided us the opportunity to investigate the effect of different substituted cobalt electrolytes on the efficiency of D149 sensitized solar cells. The D149 has a high extinction coefficient but without any longer alkoxy chains and the blocking effect of the steric groups. By using an indoline dye (D149) [67], we investigated this hypothesis that the interaction between dye and cobalt electrolyte could be effective on cell performance. The cobalt complexes and the organic dye structure applied in this study are represented in Scheme 1.

EXPERIMENTAL

Materials and Methods

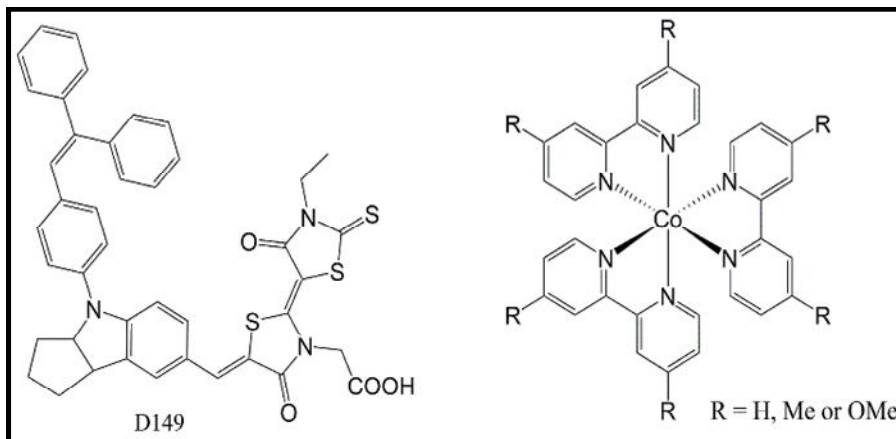
Cobalt(II) perchlorate hexahydrate, Hydrogen Chloride

Acid, Ammonium Thiocyanate, Hydrogen peroxide, lithium perchlorate, 4-tert-butylpyridine, 4,4'-Dimethyl-2,2'-dipyridyl, 4,4'-Dimethoxy-2,2'-dipyridyl, 2,2'-dipyridyl, D149 dye, Fluorine Doped Tin Oxide (FTO) glasses (~7 Ω/sq), were obtained from Sigma-Aldrich and used without further purification. The TiO₂ paste and scattering paste were purchased from Sharif Solar. All solvents including: Ethanol, Acetonitrile, Tetrahydrofuran (THF), Methanol, tert-butyl alcohol, Acetone, Toluene and Dichloromethane (DCM) were purchased from Merck.

NMR Spectroscopy (Bruker Avance II 300 MHz), UV-Vis (SPECORD S-600 and Shimadzu-2100), Ultra-Sonic (Sonics VC-750), Solar Simulator (PROVA 8300), IV Tracer (Sharif Solar IV-25) were used with the specified instruments. Cyclic voltammetry spectra were achieved with a μAutolab Type III under nitrogen atmosphere in acetonitrile solvent at scan rate of 100 mV s⁻¹. The redox electrolyte solution was 3 × 10⁻³ M [Co(L)₃(PF₆)₂] and saturated TBAPF₆ in acetonitrile. The working electrodes for CVs was a Glassy Carbon. An Ag/AgCl and Pt electrodes were employed as reference and counter electrode.

Synthesis of Cobalt Complexes

The cobalt complexes were prepared according to the literature method.[42][34] Briefly, for the synthesis of [Co(bpy)₃][PF₆]₂ and [Co(dm-bpy)₃][PF₆]₂, an equivalent amount of CoCl₂·6H₂O were dissolved in a minimum volume of methanol, followed by that, a solution of 3.3 equivalents of the bipyridine ligand in methanol added dropwise to the solution. The methanolic solution was stirred under reflux for 2 h. An excess amount of tetrabutylammonium hexafluorophosphate (TBAPF₆) was added to the mixture to precipitate the compound. The product was filtrated and washed with methanol and dried under vacuum. For the synthesis of [Co(dMO-bpy)₃][PF₆]₂ [34], an equivalent amount of CoCl₂ was added to a solution of 2 equivalents of 4,4'-dimethoxy- 2,2'-bipyridine ligand in DCM. This solution was stirred under reflux for 5 hours to form a pink compound. Then one further equivalent amount of 4,4'-dimethoxy- 2,2'-bipyridine ligand was added to the ethanolic solution containing an equivalent amount of this pink compound, and the solution was reflux for 1 h. In the next step, an excess amount of tetrabutylammonium



Scheme 1. Chemical structures of the organic dye and redox shuttles

hexafluorophosphate (TBAPF₆) was added to precipitate the product. Oxidation of cobalt complexes was accomplished by the addition of an excess amount of H₂O₂ (30% solution in water) to the acetonitrile solution of the corresponding cobalt(II) complexes. In the following, the solvent was removed by using a rotatory evaporator.

Preparation of Porous TiO₂ Photoanode

The photoanode was prepared exactly according to the previous paper [51]. The FTO glasses were washed with detergent solution, distilled water and ethanol respectively in an ultrasonic bath (each step for 10 min). Then, the FTO glasses were pretreated in 40 mM aqueous TiCl₄ solution at 60 °C for 10 min, and then again rinsed with water and ethanol. The Mesoporous TiO₂ films were deposited onto all FTO glasses by the doctor blade method. After that, the FTO glasses were dried at 125 °C for 10 min. This procedure was repeated to get a suitable thickness. In the following, a light-scattering paste was deposited with the same method. The electrodes were heated in a furnace at 325 °C for 5 min, at 375 °C for 5 min, at 450 °C for 15 min and finally at 500 °C for 15 min. Afterward, the electrodes were once again treated with 40 mM TiCl₄ solution and heated at 450 °C for 15 min and 500 °C for another 15 min. After the sintering, when TiO₂ electrodes were cooled to 80 °C, the electrodes were immersed in a dye solution containing 0.1 mM D149 in a mixture of acetonitrile and tert-butyl alcohol (volume ratio, 1:1) or toluene and kept at

room temperature overnight.

Preparation of Counter Pt-electrodes and DSSC Fabrication

The Pt-electrodes were prepared exactly according to the previous paper [51]. The FTO glasses were washed in an ultrasonic bath by using the detergent solution. The washed glasses were kept for 20 h in a 1 M solution of HCl. After draining and drying them, a 5% H₂PtCl₆ solution in 2-propanol was spin-coated on the surface of FTO glasses. Finally, they were annealed at 420 °C for 1.5 h in the atmosphere. The photoanode and Pt-counter electrode were assembled into a simple type cell. The cobalt electrolyte is consisted of 0.189 M Co(II), 0.045 M of Co(III), 0.8 M LiClO₄ and 1.3 M TBP (4-tert-butylpyridine) in a acetonitrile

RESULTS AND DISCUSSION

Spectral Properties

UV-visible spectra of the synthesized complexes in acetonitrile solution are displayed in Fig. S1. The obtained results represented that the absorption maxima of all complexes located in the UV region. However, calculated extinction coefficients at 440-450 nm for the [Co(bpy)₃][PF₆]₂, [Co(dm-bpy)₃][PF₆]₂ and [Co(dMO-bpy)₃][PF₆]₂ complexes are about $2.2 \times 10^2 \text{ M}^{-1} \text{ cm}^{-1}$, $2.7 \times 10^2 \text{ M}^{-1} \text{ cm}^{-1}$ and $2.4 \times 10^2 \text{ M}^{-1} \text{ cm}^{-1}$, respectively.

These observed extinction coefficients are very weak compared to the other redox mediators, particularly I/I_3^- .

Cyclic voltammograms of the synthesized complexes under nitrogen are represented in Fig. 1. Clearly, the Co(II)/(III) redox peaks of $[Co(dm-bpy)_3][PF_6]_{2/3}$ and $[Co(dMO-bpy)_3][PF_6]_{2/3}$ samples shift to a less positive potentials compared with $[Co(bpy)_3][PF_6]_{2/3}$. The obtained results corresponded to the presence of the electron-donating groups (methyl and methoxy) on the bipyridine ligands. It should be mentioned that the addition of the electron-donating groups to the bipyridine ligand led to increasing the electron density in the HOMO orbital of the complex, and this effect will in itself lead to enhance the electropositive character of the cobalt complexes, while it reduces the electronegativity of them [17].

Photovoltaic Properties

Effect of film thickness on the photovoltaic performance. At first, various thicknesses of the TiO_2 films were made. The effect of the thickness of the TiO_2 film on J-V curves for D149 (as sensitizer) in conjugated with synthesized $[Co(dm-bpy)_3][PF_6]_{2/3}$ electrolyte is shown in Fig. 2 and detailed photovoltaic parameters of this cell are summarized in Table 1 (J-V curves and detailed photovoltaic parameters of all cobalt cells are displayed in Fig. S2 and Table S1).

All the prepared cells were presented the best J_{SC} and efficiency at 9 μm thickness, while the V_{OC} was not changed with thickness [68]. Hagfeldt *et al.* have claimed that the photocurrent increment of the thin film of the cobalt-DSSCs is due to the high charge-collection efficiency in them, which caused a faster electron transport and slower recombination rates through the TiO_2 film [68,42]. Electron transport rate is also related to the cobalt electrolyte mass-transport, which is slower in the thick TiO_2 film. These data confirm that the thickness of the TiO_2 is very important in the DSSCs with the cobalt electrolyte and thin films improve the performance of the cobalt electrolyte in the DSSCs. So TiO_2 with the 9 μm thickness was used for further studies in this work.

Effect of dye-soaking solvent on the performance of DSSC. The I-V curves of D149/ TiO_2 cells with $[Co(dm-bpy)_3][PF_6]_{2/3}$ electrolyte with two different solvents are presented in Fig. 3 and Table 2. Interestingly, changing the

dye-soaking solvent has a considerable effect on the D149-cell. An increase in J_{sc} is observed when going from acetonitrile/ tert-butyl alcohol to toluene. This is related to the higher solubility of the dye in toluene than in acetonitrile/ tert-butyl alcohol. The amount of dye-loading was significantly increased when the toluene solvent was used. All the cobalt prepared cells were presented the best J_{SC} and efficiency in toluene solvent. Therefore, the DSSCs sensitized with D149 were prepared and optimized in toluene as dye-soaking solvent and 9 μm thickness of the TiO_2 film.

The J-V measurement of the prepared DSCs with D149 in conjugated with cobalt electrolytes are displayed in Fig. 4. The obtained data are summarized in Table 3. As a result, the V_{oc} values of the prepared cells are related to the redox potential of their complexes. Thus the difference in V_{OC} values is predominantly attributed to the differences in the redox potentials of these complexes and increase with increasing redox potential value [40,69]. For instance, the maximum V_{oc} was observed with $[Co(bpy)_3][PF_6]_{2/3}$ electrolyte, which the redox potential of this electrolyte (see voltammograms in Fig. 1) located in the more positive region compared with other complexes. Also, the obtained results represented that the J_{sc} of the $[Co(dm-bpy)_3][PF_6]_{2/3}$ and $[Co(dMO-bpy)_3][PF_6]_{2/3}$ cells increased in comparison with $[Co(bpy)_3][PF_6]_{2/3}$ cell. The J_{sc} of these cells were increased in the order of $[Co(bpy)_3][PF_6]_{2/3} < [Co(dMO-bpy)_3][PF_6]_{2/3} < [Co(dm-bpy)_3][PF_6]_{2/3}$. The bulky groups (methyl and methoxy) on the cobalt complexes can act as a spacer, and reduced the charge recombination, enhanced charge transport and improved J_{sc} .

The results are in agreement with the published outputs of Hagfeldt and co-workers that for dyes without insulating effect, the electron lifetime and recombination were dependent on the substituents on the cobalt complexes [42]. This enhancement of the J_{sc} plays an substantial role to improve the efficiency of the related cells. (see Table 3).

The best efficiency ($\eta = 4.36\%$ at 1000 Wm^{-2} irradiation) was obtained for $[Co(dm-bpy)_3][PF_6]_{2/3}$ cell with $J_{sc} = 13.81$ ($mA\ cm^{-2}$) and $V_{oc} = 546$ (mV). A similar efficiency was found by Hagfeldt and co-workers for the prepared cell with $[Co(dm-bpy)_3][PF_6]_{2/3}$ as electron-donor cobalt electrolyte and D29 dye [42]. Although the electron-donating ability and bulky effect of the methoxy-substituent

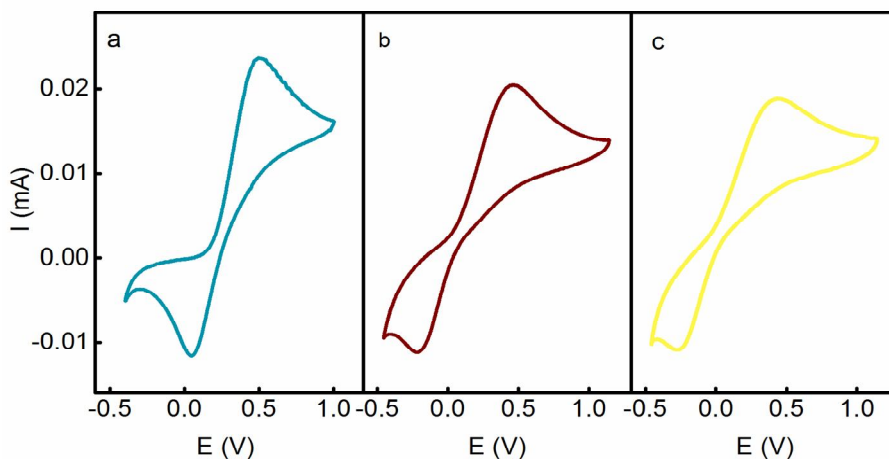


Fig. 1. Cyclic voltammogram of (a) $[\text{Co}(\text{bpy})_3][\text{PF}_6]_{2/3}$, (b) $[\text{Co}(\text{dm-bpy})_3][\text{PF}_6]_{2/3}$, (c) $[\text{Co}(\text{dMO-bpy})_3][\text{PF}_6]_{2/3}$ in acetonitrile solution with $E_{1/2}$ values 0.57, 0.41 and 0.37 V vs. NHE, respectively. The shift to a less positive potential in $[\text{Co}(\text{dm-bpy})_3][\text{PF}_6]_{2/3}$ and $[\text{Co}(\text{dMO-bpy})_3][\text{PF}_6]_{2/3}$ voltammograms compared to $[\text{Co}(\text{bpy})_3][\text{PF}_6]_{2/3}$ is attributed to the presence of electron-donating groups, methyl and methoxy. Ag/AgCl standard, platinum and glassy carbon electrodes are used as reference, counter and working electrodes.

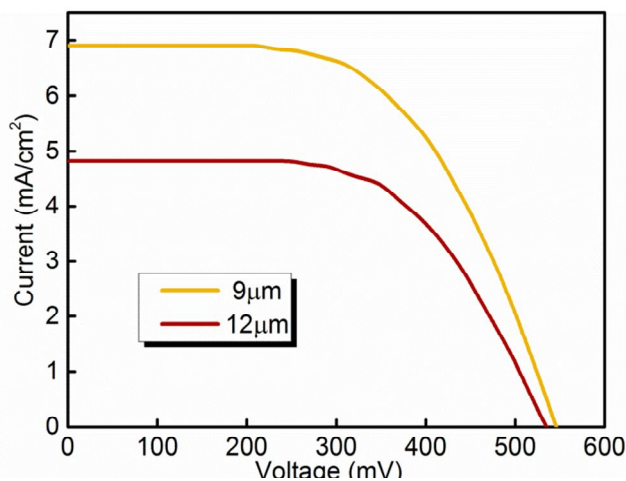


Fig. 2. J-V characteristics measured under simulated AM1.5 (1 Sun illumination) for D149 dye with different film thicknesses in conjugate with $[\text{Co}(\text{dm-bpy})_3][\text{PF}_6]_{2/3}$ electrolyte. The photocurrent decreased with increasing film thickness.

are suitable, the J_{sc} and efficiency of the prepared cell with $[\text{Co}(\text{dMO-bpy})_3][\text{PF}_6]_{2/3}$ are lower than $[\text{Co}(\text{dm-bpy})_3][\text{PF}_6]_{2/3}$ cell. It seems that the cell performance is not just dependent on the bulky group and electron-donor properties of the substituent on the redox couple. The

oxygen in the methoxy substituent is the difference between $[\text{Co}(\text{dMO-bpy})_3][\text{PF}_6]_{2/3}$ and $[\text{Co}(\text{dm-bpy})_3][\text{PF}_6]_{2/3}$ structure. This oxygen might interact with the dye and decrease the efficiency of the cell. Therefore, the structure of dye and cobalt complexes is important for their

Table 1. Photovoltaic Parameters of DSCs with Different Film thicknesses for D149 dye in Conjugate with [Co(dm-bpy)₃][PF₆]_{2/3} Electrolyte in Acetonitrile/tert-butyl Alcohol as Dye-soaking solvent

Electrolyte	TiO ₂ Thicknesses (μm)	J _{sc} (mA cm ⁻²)	V _{oc} (mV)	FF	η (%)
[Co(dm-bpy) ₃][PF ₆] _{2/3}	9	6.9	546	0.57	2.14
[Co(dm-bpy) ₃][PF ₆] _{2/3}	12	4.82	535	0.61	1.57

Table 2. Photovoltaic Parameters of DSCs with Different Solvent for D149 Dye in Conjugate with [Co(dm-bpy)₃][PF₆]_{2/3} Electrolytes

Solvent	J _{sc} (mA cm ⁻²)	V _{oc} (mV)	FF	η (%)
Acetonitrile/Tert-butyl alcohol	6.9	546	0.57	2.14
Toluene	13.81	546	0.58	4.36

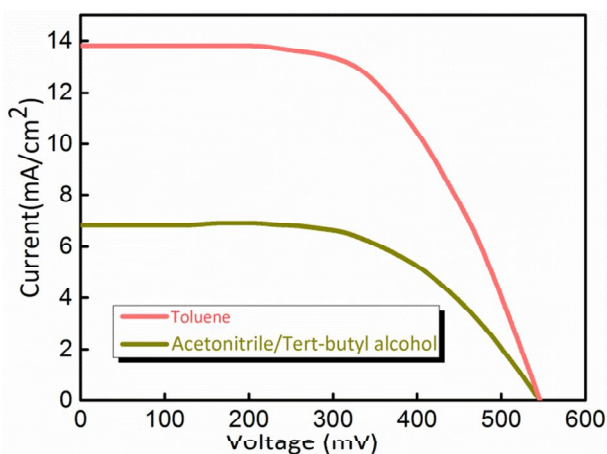


Fig. 3. Current-voltage characteristics of DSCs based on D149 dye in conjugate with [Co(dm-bpy)₃][PF₆]_{2/3} at two different dye-soaking solvents. The TiO₂ thickness was 9 μm. The photocurrent increased with toluene as dye-soaking solvent.

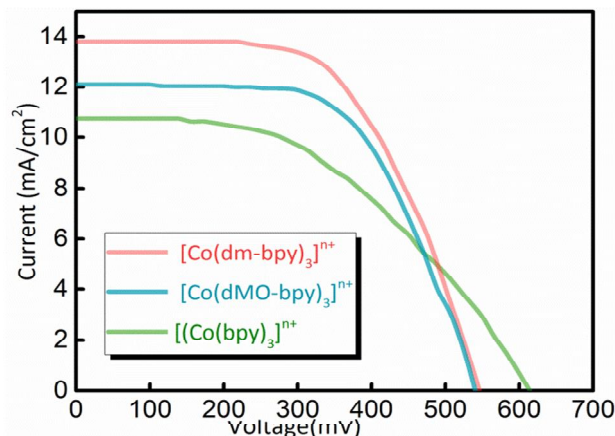


Fig. 4. J-V characteristic of D149 dye in conjugated with cobalt electrolytes.

Table 3. Photovoltaic Data of the Prepared solar cells with Different Cobalt Redox Couples by the D149 Dye and under AM1.5 G Simulated Sunlight (1000 Wm^{-2})

Electrolyte	J_{sc} (mA cm^{-2})	V_{oc} (mV)	FF	η (%)
$[\text{Co}(\text{bpy})_3][\text{PF}_6]_{2/3}$	10.75	614	0.47	3.08
$[\text{Co}(\text{dm-bpy})_3][\text{PF}_6]_{2/3}$	13.81	546	0.58	4.36
$[\text{Co}(\text{dMO-bpy})_3][\text{PF}_6]_{2/3}$	12.1	540	0.60	3.95

interaction. The optimized structure of the D149 is displayed in Fig. 5.

This dye attaches to the TiO_2 surface by a bidentate bonding, which the π system of it lay parallel to the TiO_2 surface [70-72]. From the calculation, it is known the D149 dye have a dipole moment about 10.95 ± 1 Debye and polarizability about 382.13 \AA^3 . These dipole and polarity of the dye are effective factors for interaction between cobalt complexes and the dye. The interactions between D149 dye and cobalt complex may include electrostatic interactions, hydrogen bonds or van der waals interactions. For example oxygen ionic pairs in the methoxy-group at the $[\text{Co}(\text{dMO-bpy})_3][\text{PF}_6]_{2/3}$ complex can be effectively involved with the π^* orbital of an aromatic ring (π -1p), interaction [73-75]. In

addition hydrogen atoms of cobalt complex can interact with O, S and N atoms of dye.

To gain insight about the possible interactions between the D149 dye and cobalt electrolyte, we performed a theoretical study of the D149 dye in the presence of the $[\text{Co}(\text{dm-bpy})_3]^{3+}$ and $[\text{Co}(\text{dMO-bpy})_3]^{3+}$ species with the LANL2DZ basis set. The optimized molecular structures of the adducts of D149 with $[\text{Co}(\text{dm-bpy})_3]^{3+}$ and $[\text{Co}(\text{dMO-bpy})_3]^{3+}$ species are presented in Fig. 6. The result represents the dye/electrolyte interaction between the hydrogen of the cobalt electrolyte and oxygen of D149 dye. Electron-rich sites in the dye can interact with H of the electrolyte. As shown in Fig. 6 the hydrogen of the methyl(methoxy) and aryl group from both cobalt

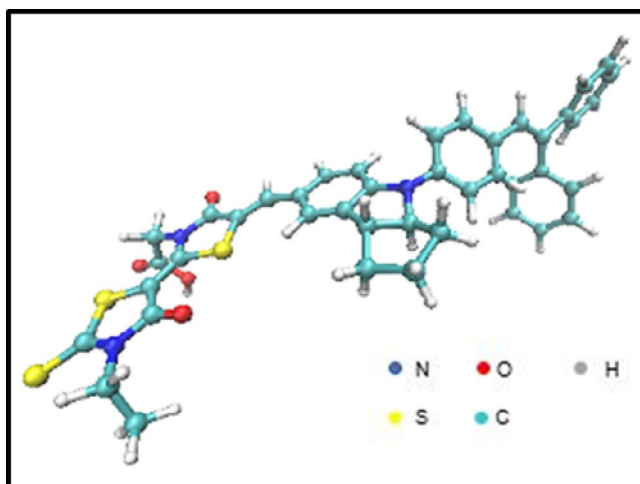


Fig. 5. The optimized structure of D149. The geometry optimization is carried out by the density functional theory (DFT) method using a hybrid functional B3LYP and 6-31G* basis set.

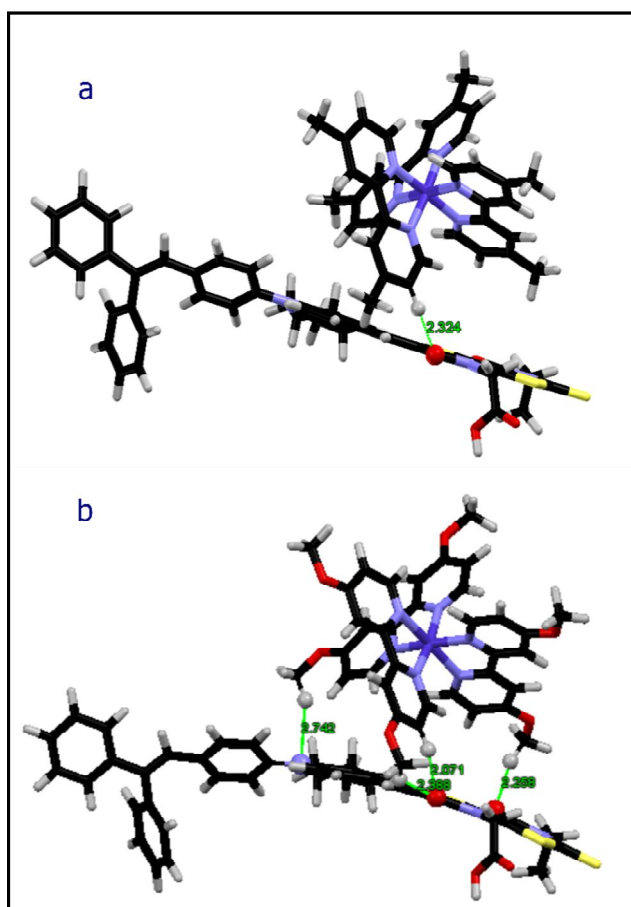


Fig. 6. Optimized molecular structures of the D149-[Co(dm-bpy)₃]²⁺ (a) D149-[Co(dMO-bpy)₃]²⁺ (b) electrolyte adducts.

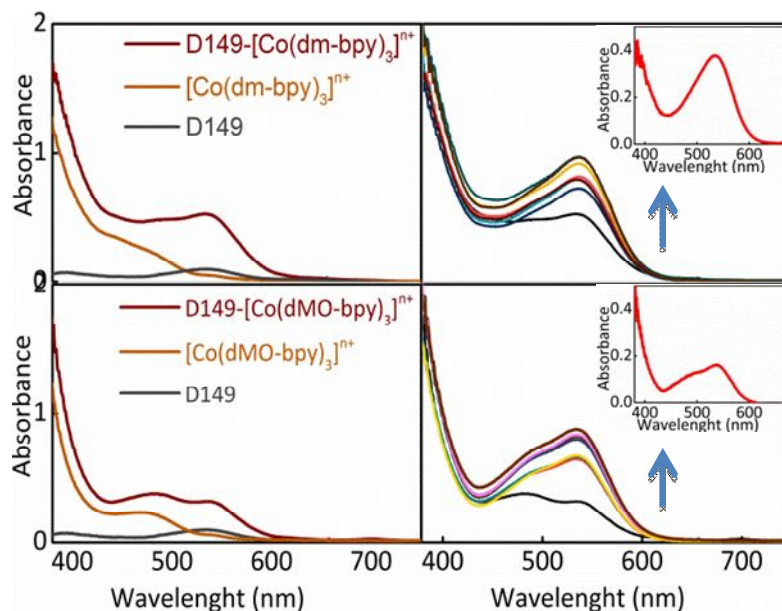


Fig. 7. UV-Vis absorbance spectra of D149 dye (9×10^{-5} M) in the presence of cobalt electrolyte (1×10^{-2} M) with molar ratio 1:1 in acetonitrile (left). Increase absorption intensity with time (right) and subtract graph.

electrolytes bind to carbonylic oxygen of the dye. According to Fig. 6 the intermolecular O---H distances are smaller than the van der Waals radii of the bonding atoms (2.72 Å) [76]. This shorter distance demonstrates an interaction between them.

The $[\text{Co}(\text{dm-bpy})_3]^{3+}$ and $[\text{Co}(\text{dMO-bpy})_3]^{3+}$ molecules interact with O atoms of the carbonyl group in the D149 dye as O---H hydrogen bonds. The number of these hydrogen bonds are four and one for $[\text{Co}(\text{dMO-bpy})_3]^{3+}$ and $[\text{Co}(\text{dm-bpy})_3]^{3+}$ molecules, respectively. Partial charge distribution of D149, $[\text{Co}(\text{dm-bpy})_3]^{3+}$ and $[\text{Co}(\text{dMO-bpy})_3]^{3+}$ molecules are shown in Fig. S3. According to the Fig. S3 the hydrogen atoms in $[\text{Co}(\text{dMO-bpy})_3]^{3+}$ are more positive than $[\text{Co}(\text{dm-bpy})_3]^{3+}$ so hydrogen atoms of $[\text{Co}(\text{dMO-bpy})_3]^{3+}$ are engaged to hydrogen interaction. Also, changing of methyl to the methoxy-substituted, one observes a slightly increased O-H interaction. Compared to the isolated D149 dye, the intramolecular C=O bonds are lengthened in the dye-electrolyte structures, representing that D149 bonds weaken upon interaction with the electrolyte. The D149- $[\text{Co}(\text{dMO-bpy})_3]^{3+}$ species show larger C-O bond distances than the D149- $[\text{Co}(\text{dm-bpy})_3]^{3+}$ species. More flexibility of the methoxy groups to that of methyl groups is responsible

for stronger interaction in D149- $[\text{Co}(\text{dMO-bpy})_3]^{3+}$ species. Consequently, these findings indicate that the intermolecular interactions of $[\text{Co}(\text{dMO-bpy})_3]^{3+}$ with D149 are more and stronger than those interactions of $[\text{Co}(\text{dm-bpy})_3]^{3+}$ with D149.

These dye-electrolyte interactions increase the concentration of the cobalt complexes near the surface and enhancing the recombination rate in the photoanode/electrolyte interface. In addition, these interactions can reduce the electron injection from the dyes to the TiO_2 by transfer of the excited electron to the electrolyte. Subsequently, the electron transfer rate decreased and the charge collection efficiency leads to a reduction of the photocurrent. Thus it seems that these interactions of electrolyte and dye is a factor for decreasing efficiency of $[\text{Co}(\text{dMO-bpy})_3][\text{PF}_6]_{2/3}$ cell compared to $[\text{Co}(\text{dm-bpy})_3][\text{PF}_6]_{2/3}$ cell.

The interaction between the dye and iodine electrolyte has already been reported [77]. O'Regan *et al.* reported the possibility of complex formation between phthalocyanine and iodine near the TiO_2 surface accelerating recombination and reducing the efficiency [78]. Also, a similar interaction was reported for ruthenium dyes/iodine [79] and ruthenium

dyes/cobalt electrolyte solar cells [80-82].

The interaction between D149 dye and cobalt complexes were investigated by UV-Vis spectroscopy and the results are displayed in Fig. 7. Spectral change (shift and intensity) can be attributed to the complex-formation in solution [83-87]. According to Figure 7, the addition of D149 solution to solution of cobalt electrolyte causes an increase in the absorbance intensity, or oscillator strength, for $[\text{Co}(\text{dm-bpy})_3]^{3+}$ -D149 and $[\text{Co}(\text{dMO-bpy})_3]^{3+}$ -D149 solutions. This hyperchromicity is indicative of the interaction between the cobalt complex and D149 dye. Type and structure of the ligands on the cobalt complexes can contribute to the interaction of the dye with electrolyte and result in the observed hyperchromism seen in the UV-Vis spectra.

In addition, the absorption intensity of spectrum increase with time for both solutions but the increase in the absorption intensity at 530 nm for $[\text{Co}(\text{dm-bpy})_3]^{3+}$ -D149 solution is larger. With subtracting cobalt and dye absorption graphs of cobalt-D149 absorption graph it can be seen that for $[\text{Co}(\text{dMO-bpy})_3]^{3+}$ -D149 solution the shape of the graph (Indicated the presence of these two species) is preserved. However for $[\text{Co}(\text{dm-bpy})_3]^{3+}$ -D149 solution, only the increases intensity of the spectrum at 530 nm is seen which is for dye and the absorbance of the electrolyte is diminished. This increase absorption at 530 for $[\text{Co}(\text{dm-bpy})_3]^{3+}$ is more pronounce than $[\text{Co}(\text{dMO-bpy})_3]^{3+}$ solution that indicated more absorption of D149 in the $[\text{Co}(\text{dm-bpy})_3]^{3+}$ -D149 solution. This phenomenon may show efficient electron transfer from $[\text{Co}(\text{dm-bpy})_3]$ electrolyte to the D149 dye and result in the more efficient cell. Hence with increase inject electron to TiO_2 film from dye, J_{sc} for $[\text{Co}(\text{dm-bpy})_3]$ increased.

CONCLUSIONS

In this study, the photoelectrochemical properties of organic dye D149 in association with cobalt-based mediators, $[\text{Co}(\text{bpy})_3][\text{PF}_6]_{2/3}$, $[\text{Co}(\text{dm-bpy})_3][\text{PF}_6]_{2/3}$ and $[\text{Co}(\text{dMO-bpy})_3][\text{PF}_6]_{2/3}$ were investigated. The results represented that the interactions between cobalt electrolytes with the dye molecules probably play a significant role in the efficiency of the cell. The chemical structures of cobalt electrolyte and D149 dye are provided the possibility for their interaction. The experimental results suggest that

efficiency order is $[\text{Co}(\text{dm-bpy})_3][\text{PF}_6]_2 > [\text{Co}(\text{dMO-bpy})_3][\text{PF}_6]_2 > [\text{Co}(\text{bpy})_3][\text{PF}_6]_{2/3}$. $[\text{Co}(\text{dMO-bpy})_3][\text{PF}_6]_2$ shows strong interaction with dye which reduces cell efficiency. $[\text{Co}(\text{dm-bpy})_3][\text{PF}_6]_2$ shows efficient electron transfer to the dye and is another factor for better performance of it. In addition, it has been shown that the thin film of TiO_2 improved performance for the cobalt cells. Hence, the best efficiency, $\eta = 4.36\%$, at 1000 Wm^{-2} irradiation was obtained for $[\text{Co}(\text{dm-bpy})_3][\text{PF}_6]_{2/3}$ cell with $J_{sc} = 13.81 \text{ (mA cm}^{-2}\text{)}$ and $V_{oc} = 546 \text{ (mV)}$. We find that the organic dyes should possess not only blocking effect for suppressing recombination properties, but also the functional group and the partial charge of dye must also be carefully engineered to prevent interaction between the dye and cobalt redox couples.

ACKNOWLEDGEMENTS

This work was supported by the Iranian National Science Foundation (INSF) and shahid Beheshti University Research Affaires.

SUPPORTING INFORMATION

UV-visible spectra of the synthesized complexes in acetonitrile solution, J-V curves and detailed photovoltaic parameters of all cobalt cells in different thickness of TiO_2 displayed in Fig. S2 and Table S1.

REFERENCES

- [1] M.Z. Iqbal, S.R. Ali, S. Khan, Solar Energy 181 (2019) 490.
- [2] A. Mahmood, Solar Energy 123 (2016) 127.
- [3] S. Rangan, S. Katalinic, R. Thorpe, R.A. Bartynski, J. Rochford, E. Galoppini, J. Phys. Chem. C 114 (2010) 1139.
- [4] P.G. Johansson, A. Kopecky, E. Galoppini, G.J. Meyer, J. Am. Chem. Soc. 135 (2013) 8331.
- [5] G.D. Sharma, D. Daphnomili, K.S. V. Gupta, T. Gayathri, S.P. Singh, P.A. Angaridis, T.N. Kitsopoulos, D. Tasis, A.G. Coutsolelos, RSC Adv. 3 (2013) 22412.
- [6] R. Hosokawa, S. Kuwahara, K. Katayama, J.

- Photochem. Photobiol. A: Chem. 334 (2017) 107.
- [7] G. Di Carlo, A.O. Biroli, F. Tessore, S. Caramori, M. Pizzotti, *Coordination Chem. Rev.* 358 (2018) 153.
- [8] Q. Liu, J. Wang, *Solar Energy* 184 (2019) 454.
- [9] S. Panagiotakis, E. Giannoudis, A. Charisiadis, R. Paravatou, M.E. Lazaridi, M. Kandyli, K. Ladomenou, P.A. Angaridis, H.C. Bertrand, G.D. Sharma, A.G. Coutsolelos, *European J. Inorg. Chem.* 2018 (2018) 2369.
- [10] V. Mallam, S. Baral, S. Gyawali, R.P. Oda, H. Elbohy, J. Nepal, Q. Qiao, M.F. Baroughi, B.A. Logue, *Solar Energy* 126 (2016) 128.
- [11] G. Di Carlo, A. Orbelli Biroli, M. Pizzotti, F. Tessore, *Frontiers in Chem.* 7 (2019).
- [12] B. Pashaei, H. Shahroosvand, M. Graetzel, M.K. Nazeeruddin, *Chem. Rev.* 116 (2016) 9485.
- [13] G.E. Zervaki, V. Tsaka, A. Vatikioti, I. Georgakaki, V. Nikolaou, G.D. Sharma, A.G. Coutsolelos, *Dalton Transactions* 44 (2015) 13550.
- [14] N. Sharifi, F. Tajabadi, N. Taghavinia, *Chem. Phys. Chem.* 15 (2014) 3902.
- [15] J. Wu, Z. Lan, J. Lin, M. Huang, Y. Huang, L. Fan, G. Luo, *Chem. Rev.* 115 (2015) 2136.
- [16] D. Saikia, Y.C. Pan, C.G. Wu, J. Fang, L.D. Tsai, H.M. Kao, *J. Mater. Chem. C* 2 (2014) 331.
- [17] L. Giribabu, R. Bolligarla, M. Panigrahi, *Chem. Record* 15 (2015) 760.
- [18] Z.S. Wang, K. Sayama, H. Sugihara, *J. Phys. Chem. B* 109 (2005) 22449.
- [19] G. Oskam, B. V Bergeron, G.J. Meyer, P.C. Searson, *J. Phys. Chem. B* 105 (2001) 6867.
- [20] T.W. Hamann, O.K. Farha, J.T. Hupp, *J. Phys. Chem. C* 112 (2008) 19756.
- [21] S. Hattori, Y. Wada, S. Yanagida, S. Fukuzumi, *J. Am. Chem. Soc.* 127 (2005) 9648.
- [22] S.C. Pradhan, A. Hagfeldt, S. Soman, *J. Mater. Chem. A* 6 (2018) 22204.
- [23] S.O. Furer, B. Bozic-Weber, T. Schefer, C. Wobill, E.C. Constable, C.E. Housecroft, M. Willger, *J. Mater. Chem. A* 4 (2016) 12995.
- [24] A. Colombo, G. Di Carlo, C. Dragonetti, M. Magni, A. Orbelli Biroli, M. Pizzotti, D. Roberto, F. Tessore, E. Benazzi, C.A. Bignozzi, L. Casarin, S. Caramori, *Inorg. Chem.* 56 (2017) 14189.
- [25] S.A Sapp, C.M. Elliott, C. Contado, S. Caramori, C.A. Bignozzi, *J. Am. Chem. Soc.* 124 (2002) 11215.
- [26] M.J. DeVries, M.J. Pellin, J.T. Hupp, *Langmuir* 26 (2010) 9082.
- [27] C. Li, S.J. Wu, C.G. Wu, *J. Mater. Chem. A* 2 (2014) 17551.
- [28] C.C. Clark, G.J. Meyer, Q. Wei, E. Galoppini, *J. Phys. Chem. B* 110 (2006) 11044.
- [29] N. Yaghoobi Nia, P. Farahani, H. Sabzyan, M. Zendehelel, M. Oftadeh, *Phys. Chem. Chem. Phys.* 16 (2014) 11481.
- [30] P. Salvatori, G. Marotta, A. Cinti, E. Mosconi, M. Panigrahi, L. Giribabu, M.K. Nazeeruddin, F. De Angelis, *Inorg. Chim. Acta* 406 (2013) 106.
- [31] M. Freitag, W. Yang, L.A. Fredin, L. D'Amario, K.M. Karlsson, A. Hagfeldt, G. Boschloo, *Chem. Phys. Chem.* 17 (2016) 3845.
- [32] T.T. Trang Pham, T.M. Koh, K. Nonomura, Y.M. Lam, N. Mathews, S. Mhaisalkar, *Chem. Phys. Chem.* 2014, pp. 1216-1221.
- [33] Y. Wang, Z. Sun, H. Wang, M. Liang, S. Xue, *J. Phys. Chem. C* 120 (2016) 13891.
- [34] M. Safdari, P.W. Lohse, L. Häggman, S. Frykstrand, D. Högberg, M. Rutland, R.A. Asencio, J. Gardner, L. Kloo, A. Hagfeldt, G. Boschloo, *RSC Adv.* 6 (2016) 56580.
- [35] R. Bondoni, A.L. Barthélémy, N. Sangiorgi, A. Sangiorgi, A. Sanson, *J. Photochem. and Photobiol. A: Chem.* 330 (2016) 8.
- [36] S. Ahmad, T. Bessho, F. Kessler, E. Baranoff, J. Frey, C. Yi, M. Grätzel, M.K. Nazeeruddin, *Phys. Chem. Chem. Phys.* 14 (2012) 10631.
- [37] J.-H. Yum, E. Baranoff, F. Kessler, T. Moehl, S. Ahmad, T. Bessho, A. Marchioro, E. Ghadiri, J.-E. Moser, C. Yi, M.K. Nazeeruddin, M. Grätzel, *Nature Commun.* 3 (2012) 631.
- [38] X.L. Zhang, W. Huang, A. Gu, W. Xiang, F. Huang, Z.X. Guo, Y.B. Cheng, L. Spiccia, *J. Mater. Chem. C* 5 (2017) 4875.
- [39] H. Nusbaumer, J. Moser, S.M. Zakeeruddin, M.K. Nazeeruddin, M. Grätzel, *J. Phys. Chem. B* 105 (2001) 10461.
- [40] M.K. Kashif, J.C. Axelson, N.W. Duffy, C.M. Forsyth, C.J. Chang, J.R. Long, L. Spiccia, U. Bach, J.

- Am. Chem. Soc. 134 (2012) 16646.
- [41] A. Aljarilla, J.N. Clifford, L. Pellejà, A. Moncho, S. Arrechea, P.D. La Cruz, F. Langa, E. Palomares, J. Mater. Chem. A 1 (2013) 13640.
- [42] S.M. Feldt, E.A. Gibson, E. Gabrielsson, L. Sun, G. Boschloo, A. Hagfeldt, J. Am. Chem. Soc. 132 (2010) 16714.
- [43] S. Mathew, A. Yella, P. Gao, R. Humphry-Baker, B.F.E. Curchod, N. Ashari-Astani, I. Tavernelli, U. Rothlisberger, M.K. Nazeeruddin, M. Grätzel, Nature Chem. 6 (2014) 242.
- [44] T.N. Murakami, N. Koumura, T. Uchiyama, Y. Uemura, K. Obuchi, N. Masaki, M. Kimura, S. Mori, J. Mater. Chem. A 1 (2013) 792.
- [45] A. Yella, S. Mathew, S. Aghazada, P. Comte, M. Grätzel, M.K. Nazeeruddin, J. Mater. Chem. C 5 (2017) 2833.
- [46] R. Jiang, A. Anderson, P.R.F. Barnes, L. Xiaoe, C. Law, B.C. O'Regan, J. Mater. Chem. A 2 (2014) 4751.
- [47] S. Soman, S.C. Pradhan, M. Yoosuf, M. V. Vinayak, S. Lingamoorthy, K.R. Gopidas, J. Phys. Chem. C (2018) acs.jpcc.8b01325.
- [48] T.N. Murakami, N. Koumura, M. Kimura, S. Mori, Langmuir 30 (2014) 2274.
- [49] Y. Liu, J.R. Jennings, Y. Huang, Q. Wang, S.M. Zakeeruddin, M. Grätzel, J. Phys. Chem. C 115 (2011) 18847.
- [50] M. Pastore, T. Etienne, F. De Angelis, J. Mater. Chem. C 4 (2016) 4346.
- [51] P. Tahay, M. Babapour Gol Afshani, A. Alavi, Z. Parsa, N. Safari, Phys. Chem. Chem. Phys. 19 (2017) 11187.
- [52] M. Miyashita, K. Sunahara, T. Nishikawa, Y. Uemura, N. Koumura, K. Hara, A. Mori, T. Abe, E. Suzuki, S. Mori, J. Am. Chem. Soc. 130 (2008) 17874.
- [53] H. Shahroosvand, S. Zakavi, A. Sousaraei, M. Eskandari, Phys. Chem. Chem. Phys. 17 (2015) 6347.
- [54] H. Shahroosvand, P. Abbasi, B.N. Bideh, Chem. Select 3 (2018) 6821.
- [55] J. Rochford, D. Chu, A. Hagfeldt, E. Galoppini, J. Am. Chem. Soc. 129 (2007) 4655.
- [56] L. Wu, J. Yu, L. Chen, D. Yang, S. Zhang, L. Han, M. Ban, L. He, Y. Xu, Q. Zhang, J. Mater. Chem. C 5 (2017) 3065.
- [57] B.C. O'Regan, K. Walley, M. Juozapavicius, A. Anderson, F. Matar, T. Ghaddar, S.M. Zakeeruddin, C. Klein, J.R. Durrant, J. Am. Chem. Soc. 131 (2009) 3541.
- [58] Z. Parsa, S.S. Naghavi, N. Safari, J. Phys. Chem. A 122 (2018) 5870.
- [59] T. Michinobu, N. Satoh, J. Cai, Y. Li, L. Han, J. Mater. Chem. C 2 (2014) 3367.
- [60] H. Shahroosvand, P. Abbasi, E. Mohajerani, M. Janghour, Dalton Transactions 43 (2014) 9202.
- [61] H. Shahroosvand, F. Nasouti, A. Sousaraei, Dalton Transactions 43 (2014) 5158.
- [62] E. Ghadiri, N. Taghavinia, S.M. Zakeeruddin, M. Gra, Fibers (2010) 1632.
- [63] S. Shogh, R. Mohammadpour, A.I. Zad, N. Taghavinia, Mater. Lett. 159 (2015) 273.
- [64] N.R. De Tacconi, W. Chanmanee, K. Rajeshwar, J. Rochford, E. Galoppini, J. Phys. Chem. C 113 (2009) 2996.
- [65] K. Ladomenou, T.N. Kitsopoulos, G.D. Sharma, A.G. Coutsolelos, RSC Adv. 4 (2014) 21379.
- [66] G.D. Sharma, G.E. Zervaki, K. Ladomenou, E.N. Koukaras, P.P. Angaridis, A.G. Coutsolelos, Journal of Porphyrins and Phthalocyanines 19 (2015) 175.
- [67] T. Horiuchi, H. Miura, K. Sumioka, S. Uchida, J. Am. Chem. Soc. 126 (2004) 12218.
- [68] X. Zong, M. Liang, C. Fan, K. Tang, G. Li, Z. Sun, S. Xue, J. Phys. Chem. C 116 (2012) 11241.
- [69] H. Nusbaumer, S.M. Zakeeruddin, J.E. Moser, M. Grätzel, Chem. - A Europ. J. 9 (2003) 3756.
- [70] M. Pastore, F. De Angelis, ACS Nano 4 (2010) 556.
- [71] T. Le Bahers, T. Pauporté, G. Scalmani, C. Adamo, I. Ciofini, Phys. Chem. Chem. Phys. 11 (2009) 11276.
- [72] W.H. Howie, F. Claeysens, H. Miura, L.M. Peter, J. Am. Chem. Soc. 130 (2008) 1367.
- [73] J.V. Alegre-Requena, E. Marques-Lopez, R.P. Herrera, ACS Catal. 7 (2017) 6430.
- [74] S.K. Singh, A. Das, Phys. Chem. Chem. Phys. 17 (2015) 9596.
- [75] B.W. Gung, Y. Zou, Z. Xu, J.C. Amicangelo, D.G. Irwin, S. Ma, H.C. Zhou, J. Org. Chem. 73 (2008) 689.

- [76] A. Bondi, Van der waals volumes and radii, *J. Phys. Chem.* 68 (1964) 441.
- [77] T. Marinado, K. Nonomura, J. Nissfolk, M.K. Karlsson, D.P. Hagberg, L. Sun, S. Mori, A. Hagfeldt, *Langmuir* 26 (2010) 2592.
- [78] B.C. O'Regan, I. López-Duarte, M.V. Martínez-Díaz, A. Forneli, J. Albero, A. Morandeira, E. Palomares, T. Torres, J.R. Durrant, *J. Am. Chem. Soc.* 130 (2008) 2906.
- [79] C.C. Clark, A. Marton, R. Srinivasan, A.A. Narducci Sarjeant, G.J. Meyer, *Inorg. Chem.* 45 (2006) 4728.
- [80] H. Torieda, K. Nozaki, A. Yoshimura, T. Ohno, *J. Phys. Chem. A* 108 (2004) 4819.
- [81] K. Omata, S. Kuwahara, K. Katayama, S. Qing, T. Toyoda, K. Lee, C. Wu, *Phys. Chem. Chem. Phys.* 17 (2015) 10170.
- [82] E. Mosconi, J.-H. Yum, F. Kessler, C.J. Gómez García, C. Zuccaccia, A. Cinti, M.K. Nazeeruddin, M. Grätzel, F. De Angelis, *J. Am. Chem. Soc.* 134 (2012) 19438.
- [83] H. Asanuma, T. Fujii, T. Kato, H. Kashida, *J. Photochem. and Photobiol. C: Photochem. Rev.* 13 (2012) 124.
- [84] H. Asanuma, T. Fujii, T. Kato, H. Kashida, *J. Photochem. Photobiol., C: Photochem. Rev.* 13 (2012) 124.
- [85] A. Arslantas, A.K. Devrim, H. Necefoglu, *Mol. Sci.* 8 (2007) 1225.
- [86] Q.L. Zhang, J.G. Liu, H. Xu, H. Li, J.Z. Liu, H. Zhou, L.H. Qu, L.N. Ji, *Polyhedron* 20 (2001) 3049.
- [87] R.S. Kumar, S. Arunachalam, *Polyhedron* 25 (2006) 3113.